Co-Channel Interference Modeling and Analysis in a Poisson Field of Interferers in Wireless Communications

Xueshi Yang and Athina P. Petropulu

Abstract—**The paper considers interference in a wireless communication network, caused by users that share the same propagation medium. Under the assumption that the interfering users are spatially Poisson distributed, and under a power-law propagation loss function, it has been shown in the past that the interference instantaneous amplitude at the receiver is α-stable distributed. Past work has not considered the second-order statistics of the interference, and has relied on the assumption that interference samples are independent. In this paper, we provide analytic expressions for the interference second-order statistics and show that, depending on the properties of the users' holding times, the interference can be correlated. We provide conditions under which the interference becomes m-dependent, ϕ-mixing or long-range dependent. Finally, we present some implications of our theoretical findings on signal detection.**

Index Terms—**Interference modeling, wireless communications, signal detection, non-Gaussian, alpha-stable distributions, long-range dependence.**

I. Introduction

IN WIRELESS communication networks, signal reception is often corrupted by interference from other sources, or users, that share the same propagation medium. Knowledge of the statistics of interference is important in achieving optimum signal detection and estimation.

Existing models for interference can be divided into two groups: empirical models and statistical-physical models. Empirical models, e.g. the hyperbolic distribution and the K-distribution [1], fit a mathematical model to the practically measured data, regardless of their physical generation mechanism. On the other hand, statistical-physical models are grounded upon the physical noise generation process. Such models include the Class A noise, proposed by Middleton [2], and the α-stable model initially proposed by Furutsu and Ishida [3], and later advanced by Giordano [4], Sousa [5], Nikias [6], Ilow [7] *et al.* A common feature in these interference models is the rate of decay of their density function, which is much slower than that of the Gaussian. Such noise is often referred to as impulsive noise.

Xueshi Yang was with ECE Department, Drexel University, Philadelphia, PA 19104. He is now with Department of Electrical Engineering, Princeton University, Princeton, NJ 08544. (e-mail: xyang@princeton.edu)

Athina P. Petropulu is with ECE Department, Drexel University, Philadelphia, PA 19104. (e-mail: athina@ece.drexel.edu)

Part of this work was presented on *IEEE - EURASIP Workshop on Nonlinear Signal and Image Processing*, Baltimore, Maryland, June, 2001 and *11th IEEE Workshop on Statistical Signal Processing*, Orchid Country Club, Singapore, August, 2001.

Impulsive noise has been observed in several indoor (cf. [8], [9]) and outdoor [2], [10] wireless communication environments. In [11], measurements of interference in mobile communication channel suggest that in some frequency ranges, impulsive noise dominates over thermal noise. Impulsive noise attains large values (outliers) more frequently than Gaussian noise. Such noise behavior has significant consequences in optimum receiver design [6], [12]. Moreover, as optimum signal detection relies on complete knowledge of the noise instantaneous and second-order statistics [13], it is important to study the spatial and/or temporal dependence structure of the noise as well as its instantaneous statistics. In the last decade, many efforts have been devoted in this direction (see for example [14], [15], [16], [17]). In [15], the authors consider a physical statistical noise model originated from antenna observations that are spatially dependent. It is shown [15] that the resulted interference can be characterized by a correlated multivariate Class A noise model. For mathematical simplicity, the temporal dependence structure has been traditionally modeled by moving average (MA) [18], or Markov models [19]. However, it is not clear whether these models have assumed a temporal dependence structure that is consistent with the physical generation mechanism of the noise. Thus, use of these models in receiver design may lead to schemes that function poorly in practice.

In this paper, we consider statistical-physical modeling for co-channel interference. In particular, we are interested in the temporal dependence structure of the interference. We adopt and extend the statistical-physical model investigated in [5], [6], [7]. The model considers a receiver, surrounded by interfering sources. The receiver picks up the superposition of all the pulses that originate from the interferers, after they have experienced power loss that is a power-law function of the distance traveled. We assume a communication network with basic waveform period T (time slot). We here focus on the interference sampled at rate $1/T$. As assumed in [5], [6], [7], at any time slot, the set of interferers forms a Poisson field in space. Assuming that from slot to slot these sets of interferers correspond to independent point processes, it was shown in [5], [6], [7] that the sampled interference constitutes an independent identically distributed (i.i.d.) α-stable process. However, the independence assumption is often violated in a practical system. To see why this would be the case, consider an interferer who starts interfering at some slot n, and remains active for a random number of slots. That interferer will still be active at time slots $n+i$, $i \in \mathbb{N}^+$, with certain probability, and will be one of the interferers at $n+i$, $i \in \mathbb{N}^+$. A direct consequence of this is that, location-wise, the interferers at time slots n and $n+i$ are not independent of each other. Independence can only be valid if the interferer remains active for at most one time slot.

In this paper, we assume that the interferer's holding time, or *session life*, is a random variable with some known distribution. We obtain the first- and second-order characteristic function of the sampled interference and show that, under certain assumptions, the interference becomes jointly α-stable. In the latter case, we give conditions for the interference to be m-dependent, ϕ-mixing or long-range dependent. In particular, if the session life is heavy-tail distributed, the interference constitutes a long-range dependent process in a generalized sense (defined in Sec.II-C). It should be noted that, in this paper, we only consider modeling of co-channel interference, which does not include thermal noise which is also present in a practical communication systems.

This paper is organized as follows. Section II provides the relevant mathematical background. Section III details the interference model. The statistics of the interference are derived in Section IV, while the dependence structure of the interference is studied in Section V. Numerical simulations are presented in Section VI. Section VII discusses some implications of long-range dependence in signal detection. Finally, Section VIII contains some concluding remarks.

II. Mathematical Background

A. Heavy-tail Distributions and α-Stable Distributions

A random variable X is *regularly-varying* with index α, if

$$P(|X| \geq x) \sim \frac{L(x)}{x^\alpha} \text{ as } x \to \infty. \tag{1}$$

Here, $L(x)$ is slowly varying function, *i.e.,* for all positive x, $\lim_{\tau\to\infty} L(\tau x)/L(\tau) = 1$ (typically such slowly varying functions are constant functions or ratios of two polynomials with identical degree). The variable X is said to be *heavy-tailed with infinite variance* if it is regularly varying with index $0 < \alpha < 2$. In those cases, the variance of X is infinite (if $\alpha < 1$ the mean and moments of order greater than or equal to α are infinite).

A particular class of heavy-tail distributions with infinite variance is the α-stable distribution. The α-stable distribution is a generalization of the Gaussian distribution. It is often classified as non-Gaussian, although it reduces to the Gaussian case when $\alpha = 2$ (to be defined). The difference between α-stable and Gaussian densities is that the tails of the former are heavier than those of the latter. Due to lack of closed form expression for their probability density functions, α-stable distributions are more conveniently characterized by their characteristic functions.

A vector $\mathbf{X} = (X_1, X_2, ..., X_d)^T$ is α-stable in $\mathbb{R}^d$, if and only if there exists a finite measure Γ on the unit sphere S_d of $\mathbb{R}^d$ and a vector $\mathbf{u}$ in $\mathbb{R}^d$, such that the characteristic function, $\Phi(\mathbf{w}) = E\exp\{j\mathbf{w}^T\mathbf{X}\}$ is given by [20]:

$$\begin{aligned}\Phi(\mathbf{w}) &= \exp\{-\int_{S_d} |(\mathbf{w},s)|^\alpha \left(1 - j\text{sign}((\mathbf{w},s))\tan\frac{\pi\alpha}{2}\right) \\ &\quad \cdot\Gamma(ds) + j(\mathbf{w},\mathbf{u})\},\end{aligned} \tag{2}$$

for $0 < \alpha \leq 2$, $\alpha \neq 1$; If $\alpha = 1$, $\tan\frac{\pi\alpha}{2}$ is replaced by $-\frac{2}{\pi}\ln|(\mathbf{w},s)|$. The parameter α is the characteristic exponent.

In the case when $d = 1$, S_1 consists of two points $\{-1\}$ and $\{1\}$, and the spectral measure Γ is concentrated on them. Correspondingly, the distribution becomes a univariate α-stable distribution, and for $\alpha \neq 1$, its characteristic function equals:

$$\begin{aligned}\Phi(\omega) &= \exp\{-|\omega|^\alpha [(\Gamma(\{1\}) + \Gamma(\{-1\})) \\ &\quad -j\text{sign}(\omega)(\Gamma(\{1\}) - \Gamma(\{-1\}))\tan\frac{\pi\alpha}{2}\Big] + j\mu\omega\Big\} \\ &\triangleq \exp\left\{-\sigma^\alpha|\omega|^\alpha(1 - j\beta\text{sign}(\omega)\tan\frac{\pi\alpha}{2}) + j\mu\omega\right\},\end{aligned}$$

where σ is the scale parameter, β is the skewness parameter, and μ is the location parameter. In short, such a univariate α-stable random variable will be denoted by $X \sim S_\alpha(\sigma,\beta,\mu)$. If $\beta = 0$, the distribution is symmetric about μ, and is termed symmetric α-stable, or simply $S\alpha S$.

B. Codifference

α-stable distributions are known for their lack of moments of order greater than or equal to α. In particular, for $\alpha < 2$, the second-order statistics do not exist. In such case, the role of covariance is played by the covariation or the codifference [20].

The codifference of two jointly $S\alpha S$, $0 < \alpha \leq 2$, random variables $\mathbf{x}_1$ and $\mathbf{x}_2$ equals:

$$R_{\mathbf{x}_1,\mathbf{x}_2} = \sigma^\alpha_{\mathbf{x}_1} + \sigma^\alpha_{\mathbf{x}_2} - \sigma^\alpha_{\mathbf{x}_1-\mathbf{x}_2} \tag{3}$$

where $\sigma_\mathbf{x}$ is the scale parameter of the $S\alpha S$ variable $\mathbf{x}$.

A quantity that is closely related to the codifference $R_{\mathbf{x}(t+\tau),\mathbf{x}(t)}$ is [20]:

$$\begin{aligned}I(\rho_1,\rho_2;\tau) &= -\ln E\{e^{j(\rho_1\mathbf{x}(t+\tau)+\rho_2\mathbf{x}(t))}\} \\ &\quad + \ln E\{e^{j\rho_1\mathbf{x}(t+\tau)}\} + \ln E\{e^{j\rho_2\mathbf{x}(t)}\}.\end{aligned} \tag{4}$$

This quantity is referred to as generalized codifference [21]. It reduces to the codifference for the case of jointly $S\alpha S$ processes, i.e.

$$R_{\mathbf{x}(t+\tau),\mathbf{x}(t)} = -I(1,-1;\tau). \tag{5}$$

$I(\rho_1,\rho_2;\tau)$ is defined for any stationary heavy-tailed random process.

C. Long-Range Dependence

A second-order process $x(t)$ is called a (wide-sense) stationary with long memory, or long-range dependence, if its autocorrelation function, $\rho(\tau)$, is finite and satisfies [22]:

$$\lim_{\tau\to\infty} \rho(\tau)/\tau^{\beta-1} = c \tag{6}$$

for some positive constant c and $\beta \in (0,1)$. From (6), it can be seen that a long-memory process is characterized by an autocorrelation that decays hyperbolically, as the lag τ increases. This is in contrast with the exponential decay corresponding to short memory processes, e.g. auto-regressive moving average(ARMA) processes.

The following generalization of the concept of long memory process can be useful for processes which lack autocorrelation.

Definition 1: [21], [23] Let $x(t)$ be a stationary process. We say that $x(t)$ is a long-memory process in a generalized sense, if $I(1,-1;\tau)$, as defined in (4), satisfies

$$\lim_{\tau\to\infty} -I(1,-1;\tau)/\tau^{\beta-1} = c \qquad (7)$$

where c is some real positive constant and $0<\beta<1$.

III. The Interference Model

In the sequel, we present the interference model, which is an extension to the model described in [5], [6], [7].

Consider a wireless communication scenario without power control, where a receiver receives the signal of interest in the presence of other interfering signals. For the sake of simplicity, we will assume that the users, which are the potential interferers, and the receiver are all on the same plane and concentrated in a disk R_b of radius b. The modeling is performed first for a finite b, and at the final step, the limit for $b\to\infty$ is taken. The three-dimensional scenario is a straightforward extension of the two-dimensional one. The receiver is placed at the origin of the coordinate system, and the users are distributed within the disk according to a two dimensional Poisson point process.

Let us define the term *emerging interferers at time interval* m, to describe the interfering sources whose contribution arrives for the first time at the receiver in the beginning of time interval m. The interferers that emerged at any time interval are located according to a Poisson point process in the space (Poisson field) with density λ. [1] It is of course reasonable to assume that the interferers that emerged at two different time slots are independent, or more precisely, correspond two independent Poisson point processes.

One issue that the model of [5], [6], [7] does not take into account is that, at time n, in addition to interferers that emerge at n, there could be interferers that emerged at some slot $m<n$, and still stay active at n. It is understood that the latter group would exist if the holding times of the users were longer than one time slot T. The combination of these two groups would make the interferers at slots m and n dependent (location-wise). We will assume that a user, once started transmission, continuously emits pulses for a duration of L time slots, where L is a random variable with known distribution.

At time n, the signal transmitted from the i-th interfering user, i.e., $p_i(t)$ propagates through the transmission medium and the receiver filters, and as a result gets attenuated and distorted. For simplicity, we assume that distortion and attenuation can be separated. Let us first consider only the filtering effect. For short time intervals, the propagation channel and the receiver can be represented by a time-invariant filter with impulse response $h(t)$. Due to filtering only, the contribution of the i-th interfering source at the receiver is of the form $x_i(t)=p_i(t)*h(t)$, where the asterisk denotes convolution. In wireless communications, the power attenuation increases logarithmically with the distance r_i between the transmitter and the receiver (cf. [2]). The power loss function can be expressed in terms of signal amplitude loss function $a(r_i)$, i.e.,

$$a(r_i)=\frac{1}{r_i^{\gamma/2}}, \qquad (8)$$

where γ is the path loss exponent; γ is a function of the antenna height and the signal propagation environment. It may vary from slightly less than 2, for hallways within buildings, to larger than 5, in dense urban environments and hard partitioned office buildings ([11]). Thus, the total signal at the receiver is:

$$x(t)=s(t)+\sum_{i\in\mathcal{N}} a(r_i)x_i(t), \qquad (9)$$

where $s(t)$ is the signal of interest, and $\mathcal{N}$ denotes the set of interferers at time t. Note that the transmitting power of user i has been implicitly incorporated into $x_i(t)$.

The receiver consists of a signal demodulator followed by the detector. A correlation demodulator decomposes the received signal into an K-dimensional vector. The signal is expanded into a series of orthonormal basis functions $\{g_k(t),\ 0<t\le T,\ k=1,...,K\}$. Let $Z_k(n)$ be the projection of $x(t)$ onto $g_k(\cdot)$ at time slot n, i.e.,

$$Z_k(n)=\int_0^T x((n-1)T+t)g_k(t)dt. \qquad (10)$$

It holds

$$Z_k(n) = S_k(n)+\sum_{i\in\mathcal{N}} a(r_i)X_{i,k}(n) \qquad (11)$$

$$\triangleq S_k(n)+Y_k(n) \qquad (12)$$

where $X_{i,k}(n)$ and $S_k(n)$ are, respectively, the result of the correlations of $x_i(t)$ and $s(t)$ with the basis functions $g_k(\cdot)$, and $Y_k(n)$ represents interference.

The $X_{i,k}(n)$'s are assumed to be spatially independent (e.g., $X_{i,k}(n)$ is independent of $X_{j,k}(n)$ for $i\neq j$). We shall focus on the statistics of $Y_k(\cdot)$ for a particular dimension k. For notational convenience, we drop the subscript k, thus denoting $Y_k(n)$ and $X_{i,k}(n)$ by $Y(n)$ and $X_i(n)$ respectively. At time n, $Y(n)$ is the sum of a random number of i.i.d. random variables, which are contributions of active interferers.

IV. Statistical Analysis of the Resulted Interference

A. Instantaneous Statistics

Now let us consider the instantaneous interference at time n. In order to calculate the instantaneous statistics, the number and locations of the active interferers at any given time interval need to be specified.

Proposition 1: Assume that the mean of the interferers' session life is finite, denoted by μ, and the density of the emerging interferers at each time slot is λ. As the sampling time n tends to infinity, the active interferers becomes Poisson distributed in the space, with asymptotic density $\lambda\mu$.

Proof: See Appendix A.

[1] λ may be a function of time and the locations of the unit area/volume, which forms a non-homogeneous Poisson point process. A non-homogeneous Poisson process can be mapped to a homogeneous one through transformations, cf. [5], [7]. In this paper, we only consider the homogeneous case, i.e. λ is a constant.

For convenience, we will set the time origin for the system considered to be $-\infty$ from now on. Therefore, at any time n, the set of active interferers form a Poisson field in the space with density $\lambda\mu$. Now we can use related results in [5], [7], where, by imposing the condition that $X_i(n)$ is symmetrically distributed, it is shown the resulted interference is $S\alpha S$ distributed (cf. Eqs. (13)-(15) in [5]). Hence, we can conclude the following Theorem.

Theorem 1: The instantaneous interference, observed at any given time interval at the receiver, is $S\alpha S$ distributed with characteristic exponent $\alpha = 4/\gamma$, and scale parameter

$$\sigma^\alpha = -\lambda\mu\pi \int_0^\infty x^{-\alpha} d\Psi(x) \tag{13}$$

were $\Psi(x)$ is the common characteristic function of $\{X_i(\cdot),\ i = 1, 2, ...\}$.

B. Joint Statistics

We next study the joint statistics of interference samples obtained at different time slots m and n. We assume $n - m = \tau > 0$.

Let us denote the interference at m and n by $Y(m)$ and $Y(n)$ respectively. It holds:

$$Y(m) = \sum_{i\in\mathcal{N}_m} a(r_i)X_i(m), \tag{14}$$

$$Y(n) = \sum_{i\in\mathcal{N}_n} a(r_i)X_i(n), \tag{15}$$

where $\mathcal{N}_m$ and $\mathcal{N}_n$ represent the set of interferers that are active at time m and n, respectively. The following proposition provides the joint characteristic function of $Y(m)$ and $Y(n)$, $\Phi_{m,n}(\omega_1, \omega_2) \triangleq \mathrm{E}\{\exp[j\omega_1 Y(m) + j\omega_2 Y(n)]\}$.

Proposition 2: Let the session life L have finite mean and we denote by $\bar{F}_L(k)$ its survival distribution function. Then, the joint characteristic function of $Y(m)$ and $Y(n)$ ($n - m = \tau > 0$) equals

$$\begin{aligned}\Phi_{m,n}(\omega_1, \omega_2) \;=\; & \exp\{-\sigma^\alpha H_1(\tau)\left(|\omega_1|^\alpha + |\omega_2|^\alpha\right) \\ & + H_2(\tau)\Theta_{m,n}(\omega_1, \omega_2)\}, \end{aligned} \tag{16}$$

where

$$\alpha = 4/\gamma, \tag{17}$$

$$\sigma = \left(-\lambda\pi \int_0^\infty x^{-\alpha} d\Psi(x)\right)^{1/\alpha}, \tag{18}$$

$$H_1(\tau) = \sum_{l=1}^{n-m} \bar{F}_L(l), \tag{19}$$

$$H_2(\tau) = \sum_{l=n-m+1}^{\infty} \bar{F}_L(l), \tag{20}$$

$$\begin{aligned}\Theta_{m,n}(\omega_1, \omega_2) \;=\; & \lim_{b\to\infty} \lambda\pi b^2 [\int_0^b \Psi_{m,n}(a(r)\omega_1, a(r)\omega_2) \\ & \cdot \frac{2r}{b^2} dr - 1]. \end{aligned} \tag{21}$$

Here, $\Psi(x)$ is the characteristic function of $X_i(\cdot)$, and $\Psi_{m,n}(\omega_1, \omega_2)$ is the second-order characteristic function of $X_i(\cdot)$, i.e.,

$$\Psi_{m,n}(\omega_1, \omega_2) = \mathrm{E}[e^{j\omega_1 X_i(m) + j\omega_2 X_i(n)}]. \tag{22}$$

Proof: see Appendix B.

C. Remarks on Proposition 2

1) Set $\omega_2 = 0$, we obtain the first order characteristic function of the interference process, i.e.,

$$\Phi(\omega_1) = e^{-\sigma^\alpha \sum_{l=1}^\infty \bar{F}_L(l)|\omega_1|^\alpha}. \tag{23}$$

Recognizing that $\sum_{l=1}^\infty \bar{F}_L(l) = \mu$, which is the mean of the session life, we get a result consistent with Theorem 1.

2) In the special case

$$\bar{F}_L(l) = \begin{cases} 1 & l = 1 \\ 0 & l > 1 \end{cases} \tag{24}$$

we have $H_2(\tau) = 0$ for $\tau = 1, 2...$, and $H_1(\tau) = 1$. Hence,

$$\ln \Phi_{m,n}(\omega_1, \omega_2) = -\sigma^\alpha \left(|\omega_1|^\alpha + |\omega_2|^\alpha\right). \tag{25}$$

Equation (25) implies that the interference samples obtained at different time slots are independent and jointly α-stable distributed. Indeed, this is consistent with the findings in [5] and [7].

3) If $H_2(\tau)$ tends to zero as τ tends to infinity, and $H_1(\tau)$ approaches the mean of session life, μ. The joint characteristic function may be simplified as

$$\lim_{\tau\to\infty} \Phi_{m,n}(\omega_1, \omega_2) = e^{-\sigma^\alpha \mu(|\omega_1|^\alpha + |\omega_2|^\alpha)}. \tag{26}$$

(26) implies that when the distance between two samples becomes asymptotically large, they are becoming independently α-stable distributed (see also Sec.V-B).

4) The loss function in (8) is a far field approximation. As r approaches zero, the power of the signal becomes infinite. Hence, it is conventional to use a truncated form

$$a(r) = \min(r^{-\gamma/2}, r_0), \tag{27}$$

for some constant $r_0 > 0$. However, such truncation leads to an intractable analytical solution. In many cases, for typical values of r_0, (8) may serve as a good approximation [5].

D. Special Cases – Jointly α-Stable Interference

It is interesting to note that, although the sampled interference is marginally α-stable, in general, it is not jointly α-stable. The latter can be verified by checking the characteristic function of (16) for general distributed $X_i(m)$. However, for some special cases of $X_i(m)$, the interference does become jointly $\alpha-$stable. We next consider two such cases.

1) $X_i(m)$ *does not vary with* m.

Such a case would arise if the $i-$th interferer remained at some constant level, B_i, throughout its session life. This may be a reasonable assumption for such interferers as discharging particles, or automobile ignition.
Let B_i be uniformly distributed between $[-1/2,\ 1/2]$. As before, let us also assume that the i-th interferer emerges at Γ_i, and its session life is L_i. The contribution from this interferer can be written as

$$X_i(m) = B_i 1_{[\Gamma_i \le m < \Gamma_i + L_i]}, \tag{28}$$

where m is integer number, and $1_{[\cdot]}$ is the indicator function. Then, it can be shown (see Appendix C) that

$$\begin{aligned}\ln \Phi_{m,n}(\omega_1, \omega_2) \\ = \quad & -\sigma^\alpha [H_1(\tau)|\omega_1|^\alpha + H_2(\tau)|\omega_1 + \omega_2|^\alpha \\ & + H_1(\tau)|\omega_2|^\alpha], \end{aligned} \tag{29}$$

where α, $H_1(\tau)$, $H_2(\tau)$ are defined as (17), (19), (20), and

$$\sigma = \left(-\lambda\pi \int_0^\infty x^{-\alpha} d\Psi_B(x) \right)^{1/\alpha} \tag{30}$$

where $\Psi_B(x)$ denotes the characteristic function of B_i. Equation (29) implies that the interference is jointly α-stable (see Appendix C).

2) *Bernoulli distributed* $X_i(m)$
In wireless communications, particularly in spread spectrum networks, most of the interference is due to co-channel users who are transmitting data sequences during their session life. A more realistic model would be to assume that the symbols are either 1 or -1 with equal probability, and independent from slot to slot.
In that case, the contribution from interferer i is

$$X_i(m) = B(m) 1_{[\Gamma_i \le m < \Gamma_i + L_i]}, \tag{31}$$

where $B(m)$ is i.i.d. Bernoulli distributed for different m, taking 1 or -1 with equal probability of $1/2$. Then, it can be shown that (see Appendix D)

$$\begin{aligned}\ln \Phi_{m,n}(\omega_1, \omega_2) \\ = \quad & -\sigma^\alpha H_1(\tau)(|\omega_1|^\alpha + |\omega_2|^\alpha) \\ & -\sigma^\alpha \frac{H_2(\tau)}{2}(|\omega_1 + \omega_2|^\alpha + |\omega_1 - \omega_2|^\alpha), \end{aligned} \tag{32}$$

where α, $H_1(\tau)$, $H_2(\tau)$ are defined as before, and

$$\sigma = \frac{1}{2} \left(\frac{\lambda \pi^{3/2} \Gamma(1 - \alpha/2)}{\Gamma(1/2 + \alpha/2)} \right)^{\frac{1}{\alpha}}. \tag{33}$$

Again, (32) implies that the interference at m and n are jointly α-stable.

V. Dependence Structure of Co-channel Interference

Eq. (16) implies that the dependence structure of the co-channel interference is determined by the session life distribution $P[L \ge k], k = 1, 2....$ In this section, we shall give conditions under which the resulted interference is m-dependent, ϕ-mixing and long-range dependent respectively. For convenience, we will focus on the case of Bernoulli distributed $X_i(m)$ (see Eq.(32)) for which the interference is jointly α-stable distributed, although it is not difficult to verify that the results presented also hold for generally distributed $X_i(m)$, provided that $\{X_i(m)\}_{m=-\infty}^{\infty}$ has finite second-order statistics for all i such that (21) is well defined.

A. *m-dependent*

A stationary random sequence $\{Y(i),\ i = 1, 2, ...\}$ is said to be m-dependent if there is a nonnegative integer m such that the sequences $\{Y(i), i = 1, ..., a\}$ and $\{Y(i), i = b, ..., \infty\}$ are statistically independent for all integers $b > a \ge 1$ satisfying $b - a > m$. For the interference model on hand, it is straightforward to show that if the maximum possible value of the session life of users is $m-1$, the interference becomes m-dependent. It lies in the fact that if $P[L \ge m] = 0$, the interferers at time instances separated more than m are independent, so is the interference.

B. *ϕ-mixing*

A more general dependence structure of importance is ϕ-mixing. ϕ-mixing defines for a stationary sequence of random variables say $\{Y(i),\ i = 1, ..., \infty\}$ satisfying the following: For $a \le b$, define $\mathcal{M}_a^b = \sigma\{Y(a), Y(a+1), \cdots, Y(b)\}$, the σ-algebra generated by the indicated random variables. Then $\{Y(i),\ i = 1, ..., \infty\}$ is ϕ-mixing if there exists a nonnegative sequence $\{\phi_i\}_{i=1}^\infty$ with $\phi_i \to 0$ such that for each k, $1 \le k < \infty$ and for each $i \ge 1$, $E_1 \in \mathcal{M}_1^k$, $E_2 \in M_{k+i}^\infty$, together imply $|P(E_1 \cap E_2) - P(E_1)P(E_2)| \le \phi_i P(E_1)$. If we also have $|P(E_1 \cap E_2) - P(E_1)P(E_2)| \le \phi_i P(E_2)$, we say that the process is *symmetrically ϕ-mixing*. Intuitively, in a ϕ-mixing process, the distant future is virtually independent of the past and the present. If $Y(i)$ is ϕ-mixing, then $e^{jY(i)}$ is also ϕ-mixing ([24], p.182). The following provides the necessary condition for the interference to be ϕ-mixing.

Proposition 3: A necessary condition for $\{Y(i),\ i = 1, ..., \infty\}$ to be ϕ-mixing is:

$$H_2(\tau) \to 0 \text{ as } \tau \to \infty, \tag{34}$$

where $H_2(\tau)$ was defined in (20).

Proof: Assuming that $Y(i)$ is ϕ-mixing, it implies ([24], Lemma 1)

$$|\mathrm{E}\{e^{jY(m)} e^{jY(n)}\} - \mathrm{E}\{e^{jY(m)}\}\mathrm{E}\{e^{jY(n)}\}| \le 2\phi_{n-m}^{1/2} \tag{35}$$

From (32), the left side of (35) is

$$\begin{aligned} & |\Phi_{m,n}(1,1) - \Phi_{m,n}(1,0)\Phi_{m,n}(0,1)| \\ = \quad & e^{-2\sigma^\alpha (H_1(\tau) + H_2(\tau))} |e^{\sigma^\alpha H_2(\tau)(2 - 2^{\alpha-1})} - 1| \\ \sim \quad & e^{-2\sigma^\alpha \mu} 2\sigma^\alpha H_2(\tau)|2 - 2^{\alpha-1}| \end{aligned} \tag{36}$$

and the result follows. □

Note that for most distributions, $H_2(\tau)$ tends to zero as $\tau \to \infty$, so that the condition is automatically satisfied.

In applications, of particular interest is the class of ϕ-mixing for which

$$\sum_n \phi_n^{1/2} < \infty. \tag{37}$$

Under this condition, samples of the ϕ-mixing noise (or their nonlinear transformations) comply with the standard central limit theorem (CLT). Such a property is useful when asymptotic convergence problem is considered. For example, in [25], to apply the asymptotic relative efficiency as a criterion for signal detection, (37) is imposed upon the ϕ-mixing noise considered.

Now, by (36), a necessary condition of (37) is given by

$$\sum_\tau H_2(\tau) < \infty, \tag{38}$$

which can be satisfied by most distributions, e.g. the exponential family.

C. Long-range dependent

In this section, we study the asymptotic dependence structure of the interference when the session life is heavy-tail distributed. In this case, condition (38) is not met. However, as we shall see, it forms another interesting class of dependence structures.

The motivation behind considering heavy-tail distributed session life is that such a distribution can well characterize many current and future communication systems. For example, in spread spectrum packet radio networks, multiple access terminals utilize the same frequency channel. The signals received at the receiver consist of superposition of the signals from all the users in the network. Assuming that multi-user detection and power-control are not implemented, the interference from other users, or otherwise referred to as self-interference, can be characterized by our interference model. As more and more wireless users are equipped with internet-enabled cell phones, their resource-request holding times (session life) are distributed with much fatter tail than that of voice only network users (cf. [26]). The session life distributions in future wireless systems are expected to be similar to the ones in current wireline networks, for which extensive statistical analysis of high-definition network traffic measurement has shown that the holding times of data network users are heavy-tailed distributed [23], [27]. In particular, they can be modelled by Pareto distributions [23], [27].

For a discrete-time communication system, we here assume that the session life is Zipf distributed (a discrete version of the Pareto distribution). A random variable X has a Zipf distribution [28] if

$$P\{X \geq k\} = [1 + (\frac{k-k_0}{\sigma})]^{-\alpha}, \;\; k = k_0, k_0+1, k_0+2... \tag{39}$$

where k_0 is an integer denoting the location parameter, $\sigma > 0$ denotes the scale parameter, and $\alpha > 0$, is the tail index. In this paper, for simplicity, we set $\sigma = k_0 = 1$, and $\alpha > 1$, which implies that $\mathrm{E}\{X\} = \zeta(\alpha)$, where $\zeta(\cdot)$ is the Riemann Zeta function. We shall denote the tail index of the session life by α_L to avoid confusion with the α defined in (17).

Since the interference is marginally heavy-tail distributed, conventional tools such as covariance that measures the dependence structure are not applicable. Instead, we use the codifference (see Eq.(4)) to explore the dependence structure.

Proposition 4: If the session life of the interferers are Zipf distributed, with tail index $1 < \alpha_L < 2$, and $X_i(m)$ are i.i.d. Bernoulli random variables taking possible values 1 and -1 with equal probability $1/2$, then, the resulted interference is long-range dependent in the generalized sense, i.e.,

$$\lim_{\tau\to\infty} \frac{-I(1,-1;\tau)}{\tau^{-(\alpha_L-1)}} = \frac{(2-2^{\alpha-1})\sigma^\alpha}{\alpha_L - 1} \tag{40}$$

where

$$\begin{aligned} \tau &: \text{ time lag between time intervals;} \\ \alpha_L &: \text{ tail index of the session life distribution;} \\ \sigma &: \text{ as defined in (33).} \end{aligned} \tag{41}$$

Proof: See Appendix E.

VI. Numerical Simulation Results

In this section, we simulate a wireless network link with Poisson distributed interferers and Bernoulli distributed $X_i(m)$'s, as described in Sec.IV-D. Our goal is to show that the simulated interference is consistent with our theoretical findings, i.e., jointly α-stable distributed with long-range dependence in the generalized sense when users' holding time is heavy-tail distributed.

The wireless communication network link was subjected to interferers which are spatially Poisson distributed over a plane with density $\lambda = 2/\pi$. The path loss was power-law with $\gamma = 4$. Once the interferers become active, they stay in the active state for random time durations, which in our simulations are Zipf [28] distributed with $k_0 = \sigma = 1$ and $\alpha_L = 1.4$. $X_i(m)$ was taken to be i.i.d. Bernoulli distributed, taking values ± 1 with equal probabilities. Then, according to (33), $\sigma = \pi$, and the instantaneous interference is $S\alpha S$ distributed with scale parameter $\sigma\mu^{1/\alpha}$, where μ is the mean of the session life. Note that $\mu = \zeta(1.4) \simeq 3.1$.

One segment of the simulated interference process is shown in Fig. 1(a) (for comparison purposes, we also simulate another trace with $\gamma = 2.2$ corresponding to $\alpha = 1.82$, as shown in Fig. 1(b). Both traces have been normalized with respect to their empirical standard deviation). As expected, it exhibits strong impulsiveness (impulsiveness becomes weaker as γ decreases, as evidenced by Fig. 1(b)). We employ the method of sample fractiles ([6] Chap. 5.3) to estimate the various parameters for the first trace (Fig. 1(a)). Assuming the data is α-stable distributed, we find that $\hat{\alpha} = 1.0044$, and scale parameter $\hat{\sigma} = 9.34$, which are very close to their theoretical value $\frac{4}{\gamma} = 1$ and 3.1π, respectively. A more rigorous statistic method to test whether the experimented data is indeed $S\alpha S$ distributed is the QQ-plot, which compares the quantiles of experimented data to those of the ideally $S\alpha S$ distributed ($\alpha = 1$) data. Should the experimental data be indeed $S\alpha S$ distributed, the QQ-plot would be linear. We synthesized ideally $S\alpha S$ distributed noise with the same parameters (α and σ) and plotted the quantiles plot versus that of the interference (length of 5000 points) in

Fig. 2. The figure clearly demonstrates that the instantaneous interference can be modeled well by the $S\alpha S$ distribution.

As shown in Sec.V-C, when the session life is heavy-tail distributed, the interference exhibits long-range dependence in the generalized sense. We estimated the codifference of the interference y_k according to [29]:

$$\widetilde{\tau}(n) = -\ln|\frac{1}{K}\sum_{k=1}^{K} e^{is(y_{k+n}-y_k)}| + \ln|\frac{1}{K}\sum_{k=1}^{K} e^{isy_{k+n}}| + \ln|\frac{1}{K}\sum_{k=1}^{K} e^{-isy_k}| \quad (42)$$

where K is the data length and s is some small multiplicative constant. 40 Monte Carlo simulations were run for the parameters described above. Each run was based on $5,000$ points and $s = 0.1$. In Fig.3(a), we overlap the estimated codifferences in a log-log scale. The linear trend is clearly seen in the graph. In Fig.3(b), we also plotted the mean (solid line) and the standard deviation (dotted line) of the estimated codifference. A least squares line was fitted to each simulation run, and the mean slope of the fitted lines is found to be -0.3829. Note that according to Proposition 4, the theoretical value is -0.4. The estimated value is in good agreement with the theory, indicating that the interference is long-range dependent in the generalized sense.

VII. Implications of Impulsive and LRD Interference

The dependence structure of the interference should be taken into account in signal detection and estimation. In particular, applying signal detection algorithms optimized for i.i.d noise to scenarios where noise is highly correlated, can yield unexpected degradation of receiver performance. This point is highlighted in the following example. We consider the problem of binary signal detection in non-i.i.d noise, but for detection, we overlook the noise dependence structure and treat it as if it were white. The consequence of ignoring the dependence is studied via the bit-error-rate (BER).

Let us assume that the transmitter is sending binary signals, $s_0 = 0$ or $s_1 = 1$ with equal probability and the transmission is corrupted by the noise n. For deciding between the two hypotheses, let us adopt the Cauchy receiver developed in [30]. It has been shown in [30] that the Cauchy receiver performs robustly in the presence of i.i.d. noise modeled as α-stable for a wide range of α, despite the fact that Cauchy noise only constitutes a special case of α-stable noise ($\alpha = 1$). Given the observation $\{x(k),\ k = 1, 2, ...\}$, the test statistic is:

$$\Lambda(k) = \frac{\gamma^2 + [x(k) - s_0(k)]^2}{\gamma^2 + [x(k) - s_1(k)]^2},\ k = 1, 2, ... \quad (43)$$

where γ is the dispersion of the interference ($\gamma = \sigma^\alpha$). If $\Lambda(k) > 1$, we decide that $s_1(\cdot)$ has been transmitted at time k, otherwise, we decide in favor of $s_0(\cdot)$.

Two different noise processes are simulated based on the proposed model, both having identical marginal distributions. In the first case, we set the session life to be Zipf distributed with $\alpha_L = 1.5$, which should lead to a long-range dependent interference. In the second case we set the session life to be equal to 1, which should result in an i.i.d. interference. Other parameters are selected such that the dispersion of the interference are the same for the two situations. Denoting the density of the interferers in first scenario by λ_1, and in second scenario by λ_2, we note that $\lambda_2 = \lambda_1\mu$, where μ is the mean the Zipf distribution.

We performed 40 Monte-Carlo simulations, with data length of 5000 each, corresponding to various values of λ. For 40 Monte-Carlo simulations, the corresponding mean BER along with the standard deviation (normalized by the mean BER) are shown in Figs.4(a) and (b) respectively. Diamond-marked lines represent the LRD case; star-marked lines are for the i.i.d. case. We observe that although the mean BER are close to each other in the two cases, there is a large discrepancy between the standard deviation of the BER. The standard deviation of the BER in the LRD case is significantly larger than in the i.i.d case. This observation implies that the highly correlated interference can degrade the performance of Cauchy receiver. This is of particular importance in practice, where finite data length is available, and where, instability of the receiver may lead to erroneous performance.

Figs. 5(a)(b) illustrate the case when α_L=1.2, vis-à-vis the i.i.d. case. λ's are chosen such that the mean BERs are similar to the previous example. It is interesting to see that, in this case, as smaller α_L implies stronger dependence, the discrepancy between the BER standard deviations further increases.

A heuristic explanation for this phenomenon lies in the observation that LRD time series exhibit strong low frequency component. There exist long periods where the maximal level tends to stay high, and also there exist long periods where the sequence stays in low levels [22]. Therefore, in a short segment of the series, one often observes cycles and trends, although the process is stationary. Thus, for signal detection in LRD interference based on finite data length, the probability of error oscillates in a wider range than in an i.i.d noise environment.

It would be of interest to study analytically the dependence of the BER statistics on the noise LRD index ($\alpha_L - 1$, see Eq. (40)). This will be subject of future investigation.

VIII. Conclusions

In this paper, we investigated the statistics of the interference resulted from a Poisson field of interferers. Key assumptions were that individual interferers have certain random session life, whose distribution is *a priori* known, and the signal propagation attenuation is power-law. We obtained the instantaneous and second order distributions of the interference. We showed that although the interference process is marginally $S\alpha S$, it is in general not jointly α-stable distributed, except in some special cases, such as the interferers sending BPSK signals, or constant amplitude signals. We provided conditions under which the interference becomes m-dependent, ϕ-mixing or long-range dependent.

The dependence structure of the interference must be taken into account to attain optimum signal detection. Some preliminary results shown in this paper indicate that, the performance of traditional detectors may deteriorate significantly under long-range dependent noise. Signal detection in the presence of impulsive and long-range dependent noise is still an open problem and is currently under investigation.

Appendix A
Proof of Proposition 1

Proof: Let $C(n)$ denote the number of active interferers at the n-th time interval. It holds

$$C(n) = \sum_k 1_{[\Gamma_k \leq n < \Gamma_k + L_k]}, \tag{44}$$

where Γ_k is the time when the sources emerged, and L_k's correspond to their session life (in multiples of T). $1_{[.]}$ is the indicator function.

Let $\bar{F}_L(\cdot)$ be the survival function of the session life, i.e.,

$$\bar{F}_L(k) \triangleq P[L \geq k],\ k = 1, 2, ... \tag{45}$$

Since the number of new interferers at each time interval is a Poisson random variable, $C(n)$ is Poisson distributed with parameter $\lambda \sum_{k=0}^{n} \bar{F}_L(n-k+1)$. Letting n tend to ∞, or alternatively, taking the time origin to be $-\infty$, the corresponding counting quantity $\widetilde{C}(n)$ asymptotically is $\lambda\mu$, where $\mu = \sum_{k=1}^{\infty} \bar{F}_L(k)$.

At any given time interval, by noting that a combined Poisson point process is still Poisson, the active interferers are spatially Poisson distributed in the space. □

Appendix B
Proof of Proposition 2

Proof: The joint characteristic function of the total interference at time m and n is:

$$\begin{aligned}\Phi_{m,n}(\omega_1, \omega_2) &= \mathrm{E}\{\exp[j\omega_1 Y(m) + j\omega_2 Y(n)]\} \\ &= \mathrm{E}\left\{\exp\left[j\omega_1 \sum_{i\in\mathcal{N}_m} a(r_i)X_i(m) \right.\right. \\ &\qquad \left.\left. + j\omega_2 \sum_{i\in\mathcal{N}_n} a(r_i)X_i(n)\right]\right\}\end{aligned} \tag{46}$$

$\mathcal{N}_m$ represents the set of interferers which are active at time m. According to their emerging time, this set can be further partitioned as:

$$\mathcal{N}_m = \bigcup_{t=-\infty}^{m} \mathcal{N}_{m,t} \tag{47}$$

where the set $\mathcal{N}_{m,t}$ contains the interferers that are active at m and emerged at time slot t. We should note here that the interferers emerged after time m will not contribute to the interference received at m. Thus the summations of the form $\sum_{i\in\mathcal{N}_m}$ can be replaced by the double summation $\sum_{t=-\infty}^{m} \sum_{i\in\mathcal{N}_{m,t}}$.

By assumption, the interferers in $\mathcal{N}_{m,t},\ t = 1, 2...$ are independent of each other for different t. The same independence conclusion applies to interferers in $\mathcal{N}_{n,t},\ t = 1, 2....$ Thus, the joint characteristic function becomes:

$$\begin{aligned}&\Phi_{m,n}(\omega_1, \omega_2) \\ &= \mathrm{E}\left\{\exp\left[\sum_{t=-\infty}^{m}\left(j\omega_1 \sum_{i\in\mathcal{N}_{m,t}} a(r_i)X_i(m)\right.\right.\right. \\ &\qquad \left. + j\omega_2 \sum_{i\in\mathcal{N}_{n,t}} a(r_i)X_i(n)\right) \\ &\qquad \left.\left. + \sum_{t=m+1}^{n} j\omega_2 \sum_{i\in\mathcal{N}_{n,t}} a(r_i)X_i(n)\right]\right\} \\ &= \prod_{t=-\infty}^{m} \mathrm{E}\left\{\exp\left[j\omega_1 \sum_{i\in\mathcal{N}_{m,t}} a(r_i)X_i(m)\right.\right. \\ &\qquad \left.\left. + j\omega_2 \sum_{i\in\mathcal{N}_{n,t}} a(r_i)X_i(n)\right]\right\} \\ &\qquad \cdot \prod_{t=m+1}^{n} \mathrm{E}\left\{\exp\left[j\omega_2 \sum_{i\in\mathcal{N}_{n,t}} a(r_i)X_i(n)\right]\right\} \qquad (48) \\ &= \prod_{t=-\infty}^{m} I_1(t) \cdot \prod_{t=m+1}^{n} I_2(t) \qquad (49)\end{aligned}$$

where the definitions of $I_1(t)$ and $I_2(t)$ can be easily deduced by (48).

We divide the calculation $I_1(t)$ and $I_2(t)$ into cases for $t < m$, $t = m$, $m < t < n$ and $t = n$ respectively.

I) $t < m$

For interferers started at time $t < m$, they can be classified into 3 groups according to their active/inactive states in m and n:

1) inactive at both m and n, i.e. their session life are shorter than $m - t + 1$. Let K_t'' denote this set of interferers;
2) active at m but not n ($m-t+1 \leq$ session life $< n-t+1$) (denoted by K_t');
3) active at both m and n (session life $\geq n-t+1$). (denoted by K_t.)

We then have, $\mathcal{N}_{m,t} = K_t' \bigcup K_t$ and $\mathcal{N}_{n,t} = \{K_t\}$. Therefore, for $t < m$,

$$\begin{aligned}I_1(t) &= \mathrm{E}\left\{\exp\left[j\omega_1\left(\sum_{i\in K_t'} + \sum_{i\in K_t}\right) a(r_i)X_i(m)\right.\right. \\ &\qquad \left.\left. + j\omega_2 \sum_{i\in K_t} a(r_i)X_i(n)\right]\right\} \\ &= \mathrm{E}\left[\exp\{j \sum_{i\in K_t} a(r_i)(\omega_1 X_i(m) + \omega_2 X_i(n))\right. \\ &\qquad \left. + j\omega_1 \sum_{i\in K_t'} a(r_i)X_i(m)\}\right].\end{aligned} \tag{50}$$

To compute (50), the sum is first taken for all sources restricted in a disk centered at the receiver, R_b, which has a radius of b. Assuming there are total k sources that started emission at time t, due to the Poisson assumption their locations are independent and uniform distributed on the disk R_b. Let us use k_t, k_t' and k_t'' to denote the number of elements in sets set K_t, K_t' and K_t'' respectively. From Eq. (50), we get:

$$\begin{aligned}
I_1(t) &= \lim_{b\to\infty}\sum_{k=0}^{\infty} P\{k \text{ sources started in } R_b \text{ at } t\} \\
&\cdot \mathrm{E}\Big[\exp\{j\sum_{i\in K_t} a(r_i)(\omega_1 X_i(m)+\omega_2 X_i(n)) \\
&+ j\omega_1 \sum_{i\in K_t'} a(r_i)X_i(m)\} | k_t + k_t' + k_t'' = k\Big] \\
&= \lim_{b\to\infty}\sum_{k=0}^{\infty} P\{k \text{ in } R_b \text{ at } t\} \\
&\cdot \mathrm{E}\Big[\prod_{i\in K_t} \mathrm{E}\left[e^{ja(r_i)(\omega_1 X_i(m)+\omega_2 X_i(n))}\right] \\
&\cdot \prod_{i\in K_t'} \mathrm{E}\left[e^{j\omega_1 a(r_i)X_i(m)}\right] | k_t + k_t' + k_t'' = k\Big] \\
&= \lim_{b\to\infty}\sum_{k=0}^{\infty} P\{k \text{ in } R_b \text{ at } t\} \\
&\mathrm{E}\Big[\prod_{i\in K_t} \Psi_{m,n}(a(r_i)\omega_1, a(r_i)\omega_2) \\
&\cdot \prod_{i\in K_t'} \Psi(a(r_i)\omega_1) | k_t + k_t' + k_t'' = k\Big], \qquad (51)
\end{aligned}$$

where $\Psi(\omega_1)$ and $\Psi_{m,n}(\omega_1,\omega_2)$ are the first and second order characteristic function of $X_i(n)$.

Since the survival function of the session life is $\bar{F}_L(\cdot)$, the probability that an interferer that emerged at time t will remain active until n is

$$P_1(n,t) = \bar{F}_L(n-t+1) \qquad (52)$$

The probability that an interferer that emerged at t will survive until m but will die out at n is

$$P_2(m,n,t) = \bar{F}_L(m-t+1) - \bar{F}_L(n-t+1), \qquad (53)$$

while the probability that an interferer will be inactive at m is

$$P_3(m,t) = 1 - \bar{F}_L(m-t+1). \qquad (54)$$

If there are k interferers beginning their emission at t, the probability that l of them are active until time n, and p of them are active at m but not n is

$$\begin{aligned}
&P\{k_t = l, k_t' = p\} \\
&= \binom{k}{l}\binom{k-l}{p} P_1(n,t)^l P_2(m,n,t)^p P_3(m,t)^{(k-l-p)} \\
&= \frac{k!}{l!p!(k-l-p)!} P_1(n,t)^l P_2(m,n,t)^p P_3(m,t)^{k-l-p} \qquad (55)
\end{aligned}$$

where $l+p \le k$.

Combining (55) and(51) we get

$$\begin{aligned}
I_1(t) &= \lim_{b\to\infty}\sum_{k=0}^{\infty}\frac{e^{-\lambda\pi b^2}(\lambda\pi b^2)^k}{k!}\sum_{l=0}^{k}\sum_{p=0}^{k-l} P\{k_t = l, k_t' = p\} \\
&\cdot \prod_{i\in K_t} \mathrm{E}\left[\Psi_{m,n}(a(r_i)\omega_1, a(r_i)\omega_2)\right] \prod_{i\in K_t'} \mathrm{E}\left[\Psi(a(r_i)\omega_1)\right] \\
&= \lim_{b\to\infty}\sum_{k=0}^{\infty}\frac{e^{-\lambda\pi b^2}(\lambda\pi b^2)^k}{k!}\sum_{l=0}^{k}\sum_{p=0}^{k-l} P\{k_t = l, k_t' = p\} \\
&\cdot \left[\int_0^b \Psi_{m,n}(a(r_i)\omega_1, a(r_i)\omega_2) f_{\mathbf{r}}(r)dr\right]^l \\
&\cdot \left[\int_0^b \Psi(a(r_i)\omega_1) f_{\mathbf{r}}(r)dr\right]^p \\
&= \lim_{b\to\infty} e^{-\lambda\pi b^2}\sum_{k=0}^{\infty}\sum_{l=0}^{k}\sum_{p=0}^{k-l}\frac{1}{l!p!(k-l-p)!}U^l V^p \\
&\cdot P_3(m,t)^{k-l-p}(\lambda\pi b^2)^k, \qquad (56)
\end{aligned}$$

where $U = P_1(n,t)\int_0^b \Psi_{m,n}(a(r)\omega_1, a(r)\omega_2) f_{\mathbf{r}}(r)dr$ and $V = P_2(m,n,t)\int_0^b \Psi(a(r)\omega_1) f_{\mathbf{r}}(r)dr$. Then, from(56) we get:

$$\begin{aligned}
I_1(t) &= \lim_{b\to\infty} e^{-\lambda\pi b^2}\sum_{k=0}^{\infty}\sum_{l=0}^{k}\sum_{p=0}^{k-l}\frac{1}{l!p!(k-l-p)!} \\
&\cdot \left[P_3(m,t)\lambda\pi b^2\right]^k \left[\frac{U}{P_3(m,t)}\right]^l \left[\frac{V}{P_3(m,t)}\right]^p \\
&= \lim_{b\to\infty} e^{-\lambda\pi b^2}\sum_{k=0}^{\infty}\sum_{l=0}^{k}\left[P_3(m,t)\lambda\pi b^2\right]^k \left[\frac{U}{P_3(m,t)}\right]^l \\
&\cdot \left[1+\frac{V}{P_3(m,t)}\right]^{k-l} / (l!(k-l)!) \\
&= \lim_{b\to\infty} e^{-\lambda\pi b^2}\sum_{k=0}^{\infty}\left[P_3(m,t)\lambda\pi b^2\right]^k \\
&\cdot \left[1+\frac{U}{P_3(m,t)}+\frac{V}{P_3(m,t)}\right]^k / k! \\
&= \lim_{b\to\infty} e^{-\lambda\pi b^2} e^{\lambda\pi b^2(P_3(m,t)+U+V)} \qquad (57)
\end{aligned}$$

The logarithm of (50) equals:

$$\begin{aligned}
&\ln I_1(t)\\
&= \lim_{b\to\infty} -\lambda\pi b^2 + \lambda\pi b^2 (P_3(m,t) + U + V)\\
&= \lim_{b\to\infty} \lambda\pi b^2 [U + V - P_1(n,t) - P_2(m,n,t)]\\
&= \lim_{b\to\infty} \lambda\pi b^2 \left[P_1(n,t)[\int_0^b \Psi_{m,n}(a(r)\omega_1, a(r)\omega_2) f_{\mathbf{r}}(r) \right.\\
&\quad \left. -1] + P_2(m,n,t)[\int_0^b \Psi(a(r)\omega_1) f_{\mathbf{r}}(r) - 1] \right]\\
&= \lim_{b\to\infty} \lambda\pi b^2 \left[P_1(n,t)[\int_0^b \Psi_{m,n}(a(r)\omega_1, a(r)\omega_2) \frac{2r}{b^2} \right.\\
&\quad \left. -1] + P_2(m,n,t)[\int_0^b \Psi(a(r)\omega_1) \frac{2r}{b^2} - 1] \right] \qquad (58)
\end{aligned}$$

Proceeding in the manner of [5], the second term in (58) can be simplified as

$$\begin{aligned}
&\lim_{b\to\infty} \lambda\pi b^2 P_2(m,n,t) \left[\int_0^b \frac{\Psi(a(r)\omega_1)}{b^2} br^2 - 1 \right]\\
&= \quad -\sigma^\alpha P_2(m,n,t)|\omega_1|^\alpha \qquad (59)
\end{aligned}$$

where

$$\sigma^\alpha = -\lambda\pi \int_0^\infty x^{-\alpha} d\Psi(x) \qquad (60)$$

Denoting

$$\begin{aligned}
&\Theta_{m,n}(\omega_1,\omega_2)\\
&= \lim_{b\to\infty} \lambda\pi b^2 \left[\int_0^b \Psi_{m,n}(a(r)\omega_1, a(r)\omega_2) \frac{2r}{b^2} dr - 1 \right],
\end{aligned}$$

we finally get:

$$\begin{aligned}
\prod_{t=-\infty}^{m-1} I_1(t) &= \prod_{t=-\infty}^{m-1} \exp\{P_1(n,t)\Theta_{m,n}(\omega_1,\omega_2)\\
&\quad -\sigma^\alpha P_2(m,n,t)|\omega_1|^\alpha\}\\
&= \exp\left\{ \sum_{t=-\infty}^{m-1} P_1(n,t)\Theta_{m,n}(\omega_1,\omega_2) \right.\\
&\quad \left. - \sum_{t=-\infty}^{m-1} \sigma^\alpha P_2(m,n,t)|\omega_1|^\alpha] \right\}. \qquad (61)
\end{aligned}$$

Let $\tau = n - m$, then,

$$\sum_{t=-\infty}^{m-1} P_1(n,t) = \sum_{t=-\infty}^{m-1} \bar{F}_L(n-t+1) = \sum_{l=\tau+2}^{\infty} \bar{F}_L(l), \quad (62)$$

and

$$\begin{aligned}
&\sum_{t=-\infty}^{m-1} P_2(m,n,t)\\
&= \sum_{t=-\infty}^{m-1} \bar{F}_L(m-t+1) - \sum_{t=-\infty}^{m-1} \bar{F}_L(n-t+1)\\
&= \sum_{l=2}^{\tau+1} \bar{F}_L(l) \qquad (63)
\end{aligned}$$

Equations (61) (62) (63) define the contributions from interferers which emerged before time m.

II) $t = m$

Interferers that emerged at time m need to be treated differently, since they always contribute to the interference at m, while not necessarily at n. Nevertheless, these interferers can be grouped as either active or inactive at n. Hence, for $t = m$, we have

$$\mathcal{N}_{m,m} = \mathcal{N}_{n,m} \bigcup \overline{\mathcal{N}}_{n,m} \qquad (64)$$

where $\overline{\mathcal{N}}_{n,m}$ represents the interferers started at m, but died out before n. We will use $k_{n,m}$ and $\bar{k}_{n,m}$ to enumerate $\mathcal{N}_{n,m}$ and $\overline{\mathcal{N}}_{n,m}$ respectively.

For $t = m$, we get

$$\begin{aligned}
I_1(m) \quad = \quad & \mathrm{E}\left[\exp\{j \sum_{i\in\mathcal{N}_{n,m}} a(r_i)(\omega_1 X_i(m) + \omega_2 X_i(n)) \right.\\
& \left. + j\omega_1 \sum_{i\in\overline{\mathcal{N}}_{n,m}} a(r_i) X_i(m)\} \right]. \qquad (65)
\end{aligned}$$

For any interferer starting at time m, it remains active until n with probability $P_{m1} = \bar{F}_L(n-m+1)$, while it ends emission before n with probability $P_{m2} = 1 - P_{m1}$. Following similar reasoning as before, we may proceed to calculate (65) as

$$\begin{aligned}
&I_1(m)\\
&= \lim_{b\to\infty} \sum_{k=0}^{\infty} P\{k \text{ in } R_b \text{ at } m\}\\
&\quad \cdot \mathrm{E}\left[\prod_{i\in\mathcal{N}_{n,m}} \mathrm{E}\left[e^{ja(r_i)(\omega_1 X_i(m) + \omega_2 X_i(n))} \right] \right.\\
&\quad \left. \cdot \prod_{i\in\overline{\mathcal{N}}_{n,m}} \mathrm{E}\left[e^{j\omega_1 a(r_i) X_i(m)} \right] | k_{n,m} + \bar{k}_{n,m} = k \right]\\
&= \lim_{b\to\infty} \sum_{k=0}^{\infty} \frac{e^{-\lambda\pi b^2}(\lambda\pi b^2)^k}{k!} \sum_{l=0}^{k} \frac{k!}{l!(k-l)!} P_{m1}^l P_{m2}^{k-l}\\
&\quad \cdot \left[\int_0^b \Psi_{m,n}(a(r)\omega_1, a(r)\omega_2) f_{\mathbf{r}}(r) dr \right]^l\\
&\quad \cdot \left[\int_0^b \Psi(a(r)\omega_1) f_{\mathbf{r}}(r) dr \right]^{k-l}\\
&= \exp\{P_{m1}\Theta_{m,n}(\omega_1,\omega_2) - \sigma^\alpha P_{m2}|\omega_1|^\alpha\}, \qquad (66)
\end{aligned}$$

where σ as defined in (60).

III) $m < t < n$

So far, we are done with the computation for interferers emerged at or before time m. Next, we are continuing with calculation of the second product term in equation (49). These interferers emerged after time m, contributing interference only at time n. Since interferers emerged between m and n may die out before n, we need to consider them separately from the interferers emerged at n.

Reasoning as before, for $m < t < n$,

$$\begin{aligned}
&\ln \prod_{t=m+1}^{n-1} I_2(t) \\
&= \sum_{t=m+1}^{n-1} \ln \lim_{b\to\infty} \sum_{k=0}^{\infty} P\{k \text{ started in } R_b \text{ at } t\} \\
&\quad \cdot \mathrm{E}\left[e^{j\omega_2 \sum_{i\in\mathcal{N}_{n,t}} a(r_i)X_i(n)} | k \text{ in } R_b\right] \\
&= \sum_{t=m+1}^{n-1} \ln \lim_{b\to\infty} \sum_{k=0}^{\infty} \frac{e^{-\lambda\pi b^2}(\lambda\pi b^2)^k}{k!} \sum_{l=0}^{k} \frac{k!}{l!(k-l)!} \\
&\quad \cdot P_1(n,t)^l (1-P_1(n,t))^{k-l} \left[\int_0^b \Psi(a(r)\omega_2) f_{\mathbf{r}}(r)\right]^l \\
&= \sum_{t=m+1}^{n-1} \lim_{b\to\infty} \lambda\pi b^2 P_1(n,t) \left(\int_0^b \Psi(a(r)\omega_2) f_{\mathbf{r}}(r) - 1\right) \\
&= -\sigma^\alpha \sum_{t=m+1}^{n-1} P_1(n,t)|\omega_2|^\alpha, \qquad (67)
\end{aligned}$$

where σ as defined before in (60).

Note that

$$\sum_{t=m+1}^{n-1} P_1(n,t) = \sum_{l=2}^{\tau} \bar{F}_L(l), \qquad (68)$$

where $\tau = n - m$.

IV) $t = n$

Finally, following similar steps, we can show that, for $t = n$,

$$\ln I_2(t) = -\sigma^\alpha |\omega_2|^\alpha. \qquad (69)$$

Plugging Eqs.(61)-(67) and (69) into (49), Eqs.(16)-(21) follow. □

APPENDIX C
PROOF OF EQ.(29)—CONSTANT CASE

We here prove Eq. (29).

Proof: We need to calculate $\Theta_{m,n}(\omega_1,\omega_2)$. Eq. (28) gives us

$$\begin{aligned}
\Psi_{m,n}(\omega_1,\omega_2) &= \mathrm{E}[e^{j\omega_1 X_i(m)+j\omega_2 X_i(n)}] \\
&= \mathrm{E}[e^{j(\omega_1+\omega_2)B_i}] \\
&= \Psi(a(r)(\omega_1+\omega_2)). \qquad (70)
\end{aligned}$$

Since,

$$\begin{aligned}
&\Theta_{m,n}(\omega_1,\omega_2) \\
&= \lim_{b\to\infty} \lambda\pi b^2 [\int_0^b \frac{\Psi(a(r)(\omega_1+\omega_2))}{b^2} dr^2 - 1] \\
&= -\sigma^\alpha |\omega_1+\omega_2|^\alpha, \qquad (71)
\end{aligned}$$

plugging (71) into (16), we obtain (29).

Next, we show that $Y(m)$ and $Y(n)$ are jointly α-stable. To see this, noting that $Y(m)$ and $Y(n)$ are symmetrically α-stable, we only need to show that the linear combination $a_1Y(n) + a_2Y(m)$ is symmetrically α-stable for any real number a_1, a_2 (Theorem 2.1.5 [20]). The log-characteristic function of the random variable $a_1Y(n) + a_2Y(m)$ equals:

$$\begin{aligned}
\ln \Phi(\omega) &= \ln \mathrm{E}\{\exp(j\omega(a_1Y(n) + a_2Y(m)))\} \\
&= \ln \Phi_{m,n}(\omega a_1, \omega a_2) \\
&= -\sigma^\alpha [H_1(\tau)|a_1|^\alpha + H_2(\tau)|a_1+a_2|^\alpha \\
&\quad + H_1(\tau)|a_2|^\alpha]|\omega|^\alpha \qquad (72)
\end{aligned}$$

which indeed is symmetrically α-stable.

□

APPENDIX D
PROOF OF EQ.(32)—BERNOULLI CASE

The characteristic function of a Bernoulli random variable, which takes 1 or -1 with equal probability $1/2$, is $\cos\omega$. Hence,

$$\begin{aligned}
\Psi_{m,n}(\omega_1,\omega_2) &= \mathrm{E}[e^{j\omega_1 X_i(m)+j\omega_2 X_i(n)}] \\
&= \cos\omega_1 \cos\omega_2. \qquad (73)
\end{aligned}$$

In the equation above, we have used the fact that $X_i(m)$ is independent of $X_i(n)$ for $m \neq n$.

Therefore, we have

$$\begin{aligned}
&\Theta_{m,n}(\omega_1,\omega_2) \\
&= \lim_{b\to\infty} \lambda\pi b^2 [\int_0^b \frac{\Psi_{m,n}(a(r)\omega_1, a(r)\omega_2)}{b^2} dr^2 - 1] \\
&= \lim_{b\to\infty} \lambda\pi b^2 [\int_0^b \cos(r^{-\gamma/2}\omega_1)\cos(r^{-\gamma/2}\omega_2) \frac{2r}{b^2} dr - 1] \\
&= \lambda\pi \int_0^\infty \left(\frac{1}{2}\cos(\omega_1+\omega_2) r^{-\gamma/2}\right. \\
&\quad \left. + \frac{1}{2}\cos(\omega_1-\omega_2) r^{-\gamma/2} - 1\right) 2r dr \\
&= \frac{\lambda\pi}{2} \int_0^\infty (\Psi(a(r)(\omega_1+\omega_2)) - 1)\, dr^2 \\
&\quad + \frac{\lambda\pi}{2} \int_0^\infty (\Psi(a(r)(\omega_1-\omega_2)) - 1)\, dr^2 \\
&= -\frac{\sigma^\alpha}{2} (|\omega_1+\omega_2|^\alpha + |\omega_1-\omega_2|^\alpha) \qquad (74)
\end{aligned}$$

where $\alpha = 4/\gamma$ and σ is defined as in (60), which can be calculated as:

$$\begin{aligned}
\sigma &= \left(-\lambda\pi \int_0^\infty x^{-\alpha} d\Psi(x)\right)^{\frac{1}{\alpha}} \\
&= \left(-\lambda\pi \int_0^\infty x^{-\alpha} d\cos(x)\right)^{\frac{1}{\alpha}}. \qquad (75)
\end{aligned}$$

The above integral exists as long as $0 < \alpha < 2$ [31]. Using the integral identity

$$\int_0^\infty x^{-\alpha} \sin x dx = \frac{\sqrt{\pi} 2^{-\alpha} \Gamma(1 - 1/2\alpha)}{\Gamma(1/2 + 1/2\alpha)}, \qquad (76)$$

we have

$$\sigma = \frac{1}{2} \left(\frac{\lambda\pi^{3/2}\Gamma(1-\alpha/2)}{\Gamma(1/2+\alpha/2)}\right)^{\frac{1}{\alpha}}. \qquad (77)$$

Now, (32) is readily verified.

APPENDIX E PROOF OF PROPOSITION 4

Proof: The codifference of the interference separated by τ can be calculated as

$$\begin{aligned} -I(1,-1;\tau) \\ &= \ln E\{e^{j(x(t+\tau)-x(t))}\} - \ln E\{e^{jx(t+\tau)}\} \\ &\quad - \ln E\{e^{-jx(t)}\} \\ &= \ln \Phi_{t,t+\tau}(-1,1) - \ln \Phi_{t,t+\tau}(0,1) - \ln \Phi_{t,t+\tau}(-1,0) \\ &= (2-2^{\alpha-1})\sigma^\alpha H_2(\tau) \end{aligned} \quad (78)$$

Plugging (39), we get

$$-I(1,-1;\tau) = (2-2^{\alpha-1})\sigma^\alpha \sum_{l=\tau+1}^{\infty} l^{-\alpha_L}. \quad (79)$$

Note that

$$\sum_{l=\tau+1}^{\infty} l^{-\alpha_L} \leq \int_{\tau+1}^{\infty} (t-1)^{-\alpha_L} dt = \frac{\tau^{-\alpha_L+1}}{\alpha_L - 1} \quad (80)$$

and

$$\sum_{l=\tau+1}^{\infty} l^{-\alpha_L} \geq \int_{\tau+1}^{\infty} t^{-\alpha_L} dt = \frac{(\tau+1)^{-\alpha_L+1}}{\alpha_L - 1}. \quad (81)$$

Since the upper bound (80) and lower bound (81) converge as $\tau \to \infty$, we conclude that

$$\lim_{\tau\to\infty} \frac{-I(1,-1;\tau)}{\tau^{-\alpha_L+1}} = \frac{(2-2^{\alpha-1})\sigma^\alpha}{\alpha_L - 1} \quad (82)$$

where σ is as given as in (33). Note that, for $\alpha \in (0,2)$, $2-2^{\alpha-1}$ and σ are positive. Hence, for $\alpha_L > 1$, $\frac{(2-2^{\alpha-1})\sigma^\alpha}{\alpha_L-1}$ is positive, and the interference process is long-range dependent in the generalized sense. □

ACKNOWLEDGEMENT

We would like to thank Dr. Steve Lowen at Harvard Medical School for the interesting discussions on Proposition 4. We also thank the anonymous reviewers for the careful reading of earlier versions of this paper.

REFERENCES

[1] E.J. Wegman, S.C.Schwartz, and J.B. Thomas, eds., *Topics in Non-Gaussian Signal Processing*, New York: Springer, 1989.

[2] D. Middleton, "Statistical-Physical Models of Electromagnetic Interference,", *IEEE Trans. Electromagnetic Compatibility*, Vol.EMC-19, No3, Aug. 1977.

[3] K. Furutsu and T. Ishida, "On the theory of amplitude distribution of impulsive random noise," *J. Applied Physics*, Vo.32, No.7, 1961.

[4] A. Giordano and F. Haber, "Modeling of atmosphere noise", *Radio Science*, Vol.7, No.11, Nov., 1972.

[5] E.S. Sousa, "Performance of a spread spectrum packet radio network link in a Poisson field of interferers", *IEEE Trans. on Info. Theo.*, Vol. 38, No.6, Nov. 1992.

[6] C. L. Nikias and M. Shao, *Signal Processing with Alpha-Stable Distributions and Applications,* New York: Wiley, 1995.

[7] J. Ilow, D. Hatzinakos, "Analytic alpha-stable noise modeling in a Poisson field of interferers or scatters", *IEEE Trans. Sig. Proc.*, Vol.46, No.6, Jun. 1998.

[8] K. L. Blackard, T. S. Rappaport, and C. W. Bostian, "Measurements and models of radio frequency impulsive noise for indoor wireless communications," *IEEE J. Select. Areas Commun.,* vol. 11, no.7, pp. 991-1001, Sept. 1993.

[9] T. K. Blankenship, D. M. Krizman, and T. S. Rappaport, "Measurements and simulation of radio frequency impulsive noise in hospitals and clinics," in *Proc. 47th IEEE Veh. Technol. Conf.,* vol. 3, pp. 1942-1946, Phoenix, AZ, May 1997.

[10] S. M. Kogon and D. G. Manolakis, "Signal modeling with self-similar α-stable processes: The fractional levy stable motion model," *IEEE Trans. Sig. Processing,* Vol. 44, pp. 1006-1010, Apr. 1996.

[11] J. D. Parsons, *The Mobile Radio Propagation Channel*, New York:Wiley, 1996.

[12] S.A. Kassam, *Signal Detection in Non-Gaussian Noise*, Springer-Verlag, New York, 1987.

[13] H. V. Poor and J. B. Thomas, "Signal detection in dependent non-Gaussian noise", in *Advances in Statistical signal processing*, vol. 2, H. V. Poor and J. B. Thomas Eds., Greenwich, CT: JAI Press, 1993.

[14] P.A. Delaney, "Signal detection in multivariate Class A interference", *IEEE Trans. Commun.*, vol. 43, no. 2/3/4, Feb./Mar./Apr. 1995.

[15] K. F. McDonald and R. S. Blum, "A statistical and physical mechanisms-based interference and noise model for array observations," *IEEE Trans. Sig. Proc.*, vol. 48, no. 7, pp. 2044-2056, July 2000.

[16] D. Middleton, "Threshold detection in correlated non-Gaussian noise fields," *IEEE Trans. Inform. Theory*, vol. 41, no. 4, July 1995.

[17] X. Yang and A. P. Petropulu, "Interference modeling in radio communication networks," *Trends in Wireless Indoor Networks, Wiley Encyclopedia of Telecommunications,* J. Proakis Eds, John Wiley and Sons, New York, 2002.

[18] A. M. Maras, "Locally optimum detection in moving average non-Gaussian noise," *IEEE Trans. Commun.*, vol. 36, no. 8, pp. 907-912, Aug. 1988.

[19] A. M. Maras, "Locally optimum Bayes detection in ergotic Markov noise," *IEEE Trans. Inform. Theory*, vol. 40, no. 1, pp. 41-55, Jan. 1994.

[20] G. Samorodnitsky and M. S. Taqqu, *Stable Non-Gaussian Random processes: Stochastic Models with Infinite Variance,* New York: Chapman and Hall, 1994.

[21] A.P. Petropulu, J-C. Pesquet and X. Yang, "Power-law shot noise and relationship to long-memory processes," *IEEE Trans. on Sig. Proc.*, Vol.48, No.7, July 2000.

[22] J. Beran, *Statistics for Long-Memory Processes*, Chapman & Hall, New York, 1994.

[23] X. Yang and A.P. Petropulu, "The extended alternating fractal renewal process for modeling traffic in high-speed communication networks", *IEEE Trans. Sig. Proc.*, Vol.49, No.7, July, 2001.

[24] P. Billingsley, *Convergence of Probability Measures*, New York: Wiley, 1968.

[25] D.R. Halverson and G. L. Wise, "Discrete-Time Detection in ϕ-Mixing Noise," *IEEE Trans. Inform. Theory*, Vol. IT-26, No.2, pp.189-198, Mar. 1980.

[26] T. Kunz, T. Barry, X. Zhou *et al*, "WAP traffic: description and comparison to WWW traffic," *Proc. of 3rd ACM international Workshop on Modeling, Analysis and Simulation of Wireless and Mobile Systems*, Boston, USA, Aug. 2000.

[27] W. Willinger, M.S. Taqqu, R. Sherman, and D.V. Wilson, "Self-similarity through high-variability: statistical analysis of Ethernet LAN traffic at the source level," *IEEE/ACM Trans. Networking*, Vol.5, No.1, Feb. 1997.

[28] B.C. Arnold, *Pareto Distributions*, International Co. Publishing House, Maryland, 1983.

[29] X. Yang, A.P. Petropulu, and J.-C. Pesquet, "Estimating long-range dependence in impulsive traffic flows,", *Proc. of ICASSP 01*, Salt Lake City, UT, 2001.

[30] G.A. Tsihrintzis and C.L. Nikias, "Performance of optimum and suboptimum receivers in the presence of impulsive noise modeled as an alpha-stable process", *IEEE Trans. Comm*, Vo.43, No.2/3/4, Feb/March/April, 1995.

[31] I.S. Gradshteyn, I.M. Ryzhik, A. Jeffrey, Eds., *Table of Integrals, Series and Products*, New York: Academic Press, 1994.

Xueshi Yang received B.Sc. degree from the Electronic Engineering Department, Tsinghua University, Beijing, China, in 1998 and the Ph.D. degree in electrical engineering from Drexel University, Philadelphia, PA, in 2001.

During September 1999 - April 2000, he was a visiting researcher at Laboratoire des Signaux et Systemes, CNRS-Universit Paris Sud, SUPELEC, France. Since 2002, he has been with the Electrical Engineering Department, Princeton University, Princeton, NJ, where he is a Postdoctoral Research Associate. His research interests are in the areas of non-Gaussian signal processing for communications, fractional-order statistics and communication system modeling and analysis.

Athina P. Petropulu received the Diploma in Electrical Engineering from the National Technical University of Athens, Greece in 1986, the M.Sc. degree in Electrical and Computer Engineering in 1988 and the Ph.D. degree in Electrical and Computer Engineering in 1991, both from Northeastern University, Boston, MA.

In 1992, she joined the Department of Electrical and Computer Engineering at Drexel University where she is now a Professor. During the academic year 1999/2000 she was an Associate Professor at LSS, CNRS-Universit Paris Sud, cole Suprieure d'Electrcit in France. Dr. Petropulu's research interests span the area of statistical signal processing, communications, higher-order statistics, fractional-order statistics and ultrasound imaging. She is the co-author of the textbook entitled, "Higher-Order Spectra Analysis: A Nonlinear Signal Processing Framework," (Englewood Cliffs, NJ: Prentice-Hall, Inc., 1993). She is the recipient of the 1995 Presidential Faculty Fellow Award. She has served as an associate editor for the IEEE Transactions on Signal Processing and the IEEE Signal Processing Letters. She is a member of the IEEE Conference Board and the Technical Committee on Signal Processing Theory and Methods.

LIST OF FIGURES

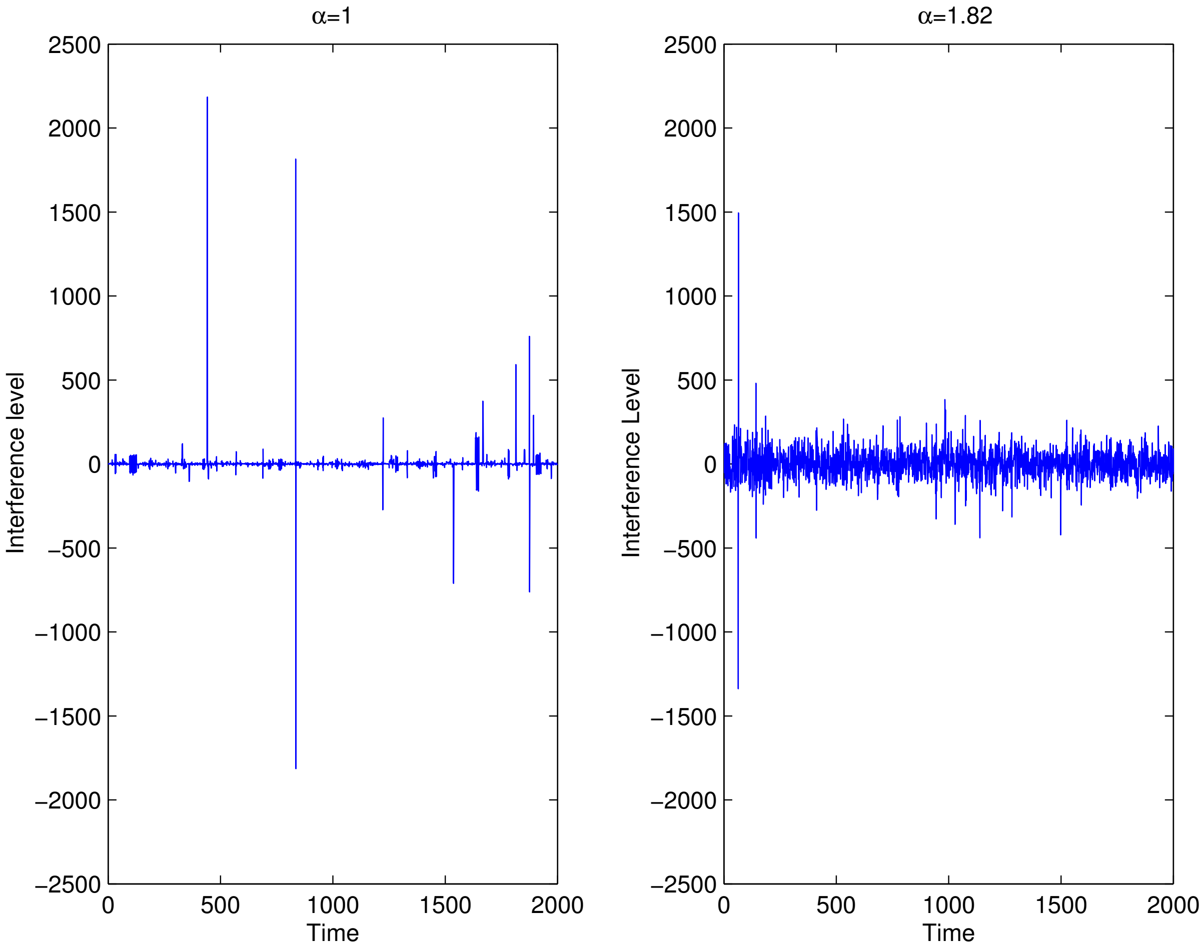

Fig. 1. Interference presented in a communication link in a Poisson field of interferers: (a) $\alpha = 1$; (b) $\alpha = 1.82$.

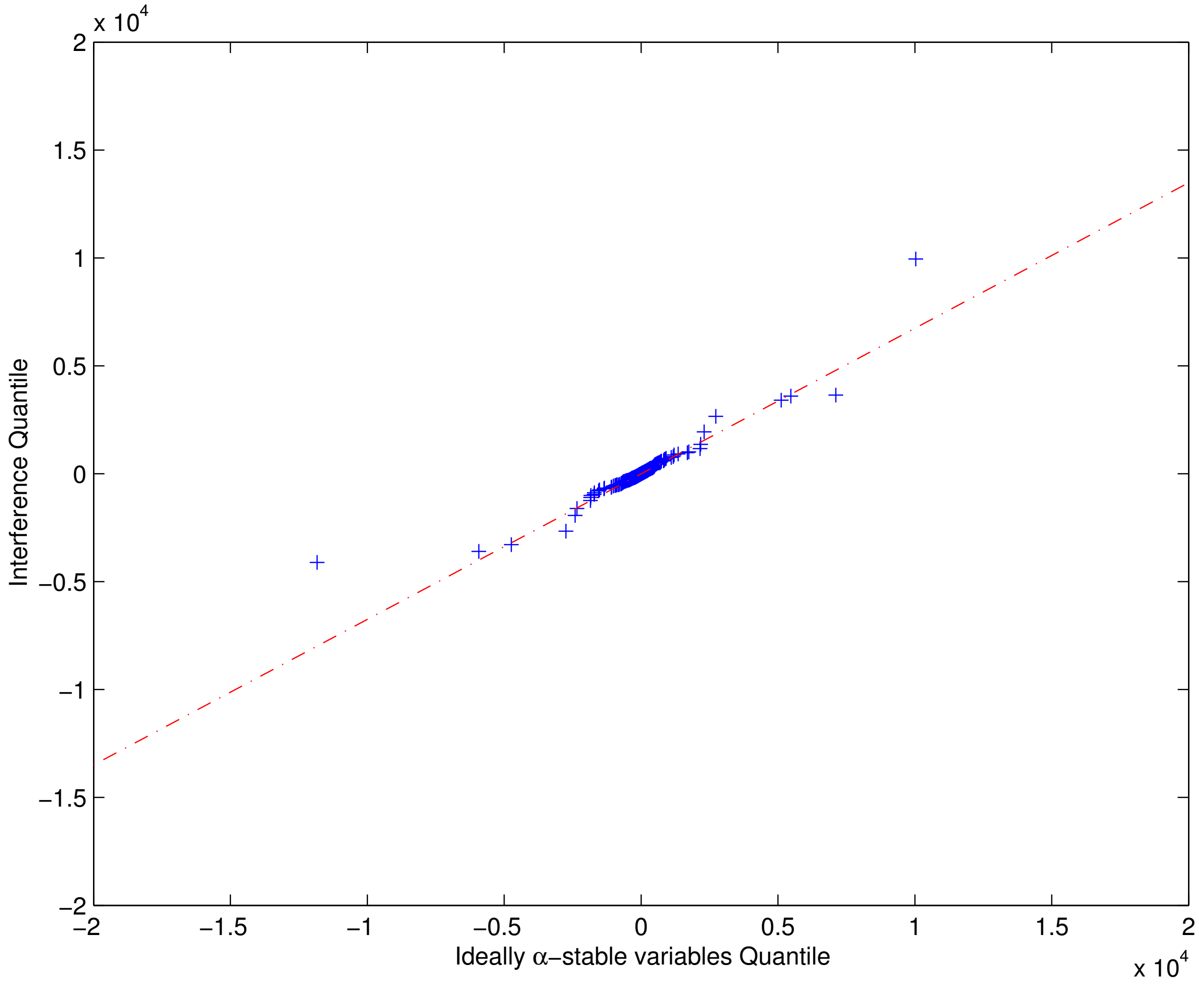

Fig. 2. QQ-plot of simulated interference and ideally $S\alpha S$ distributed random variable with the same parameter. $\alpha = 1$, which is the Cauchy distribution.

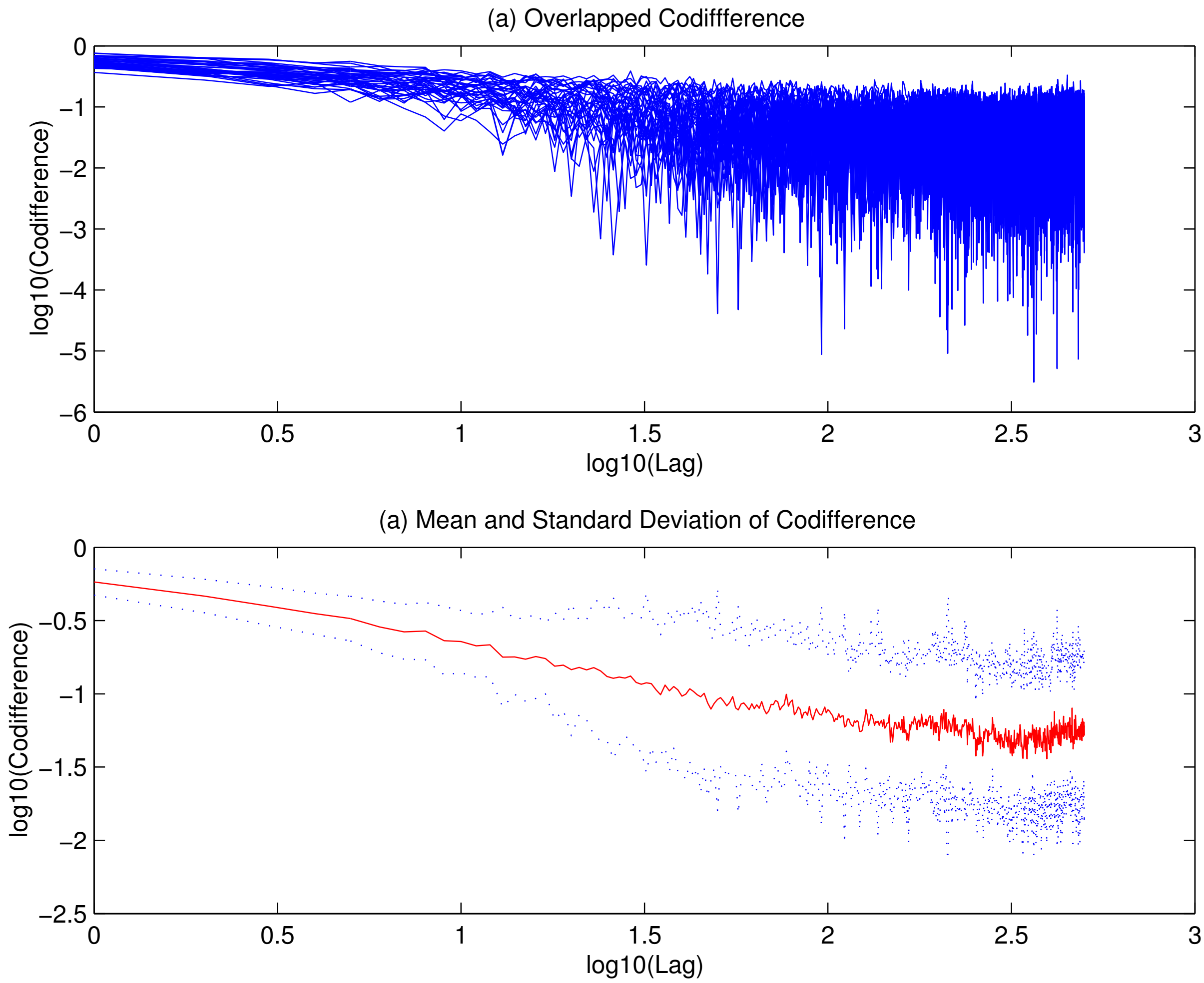

Fig. 3. (a) Log-log plot of the codifference of the interference in 40 Monte Carlo simulations. (b) Mean (solid line) and standard deviation (dotted lines)of the codifference.

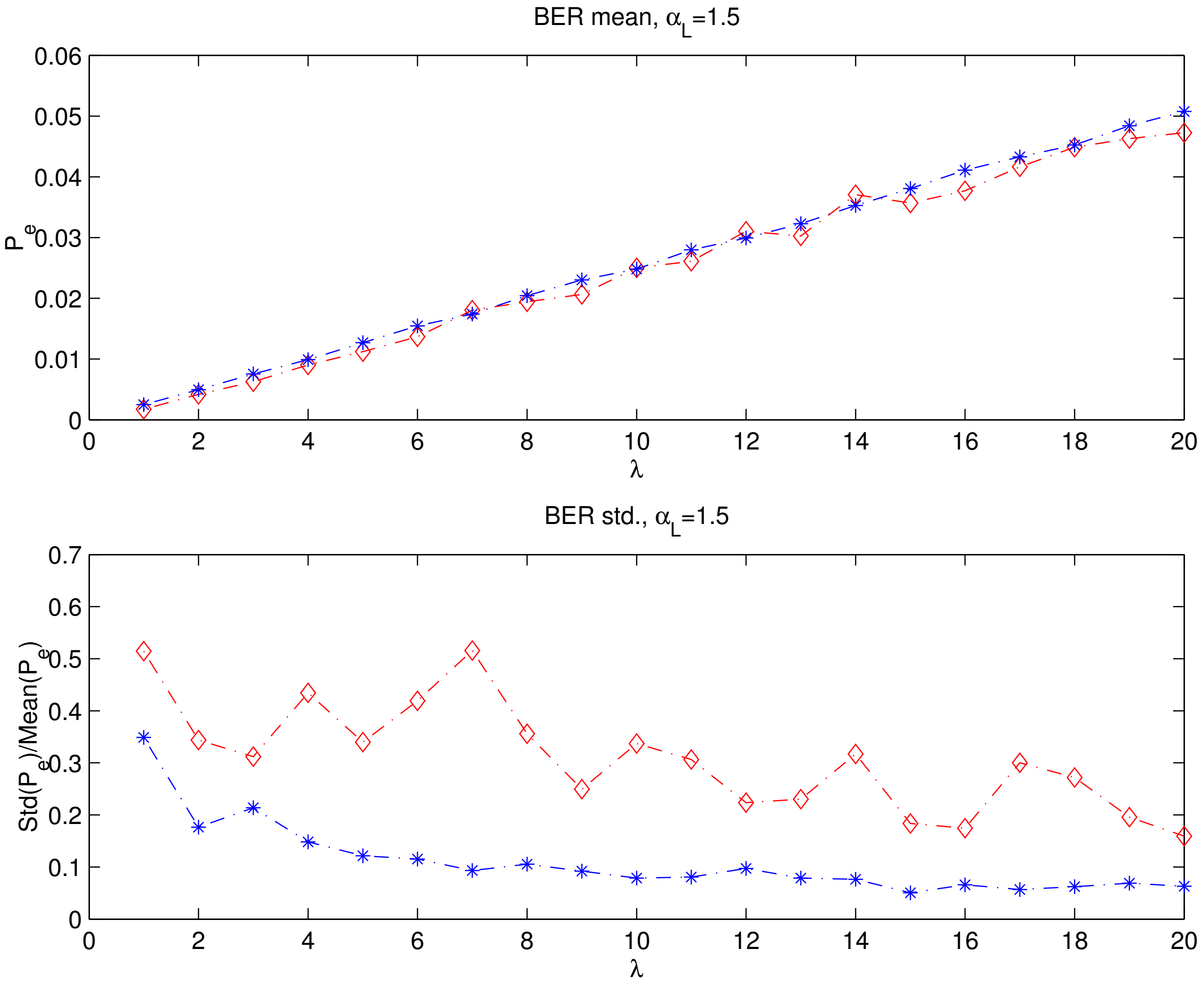

Fig. 4. Mean and standard deviation (normalized by mean) of bit-error-rate of Cauchy receiver in the presence of long-range dependent ($\alpha_L = 1.5$) and i.i.d α-stable noise, for 40 Monte Carlo simulations. Diamond-marked lines represent the long-range dependent case, while star-marked lines denote the i.i.d. case.

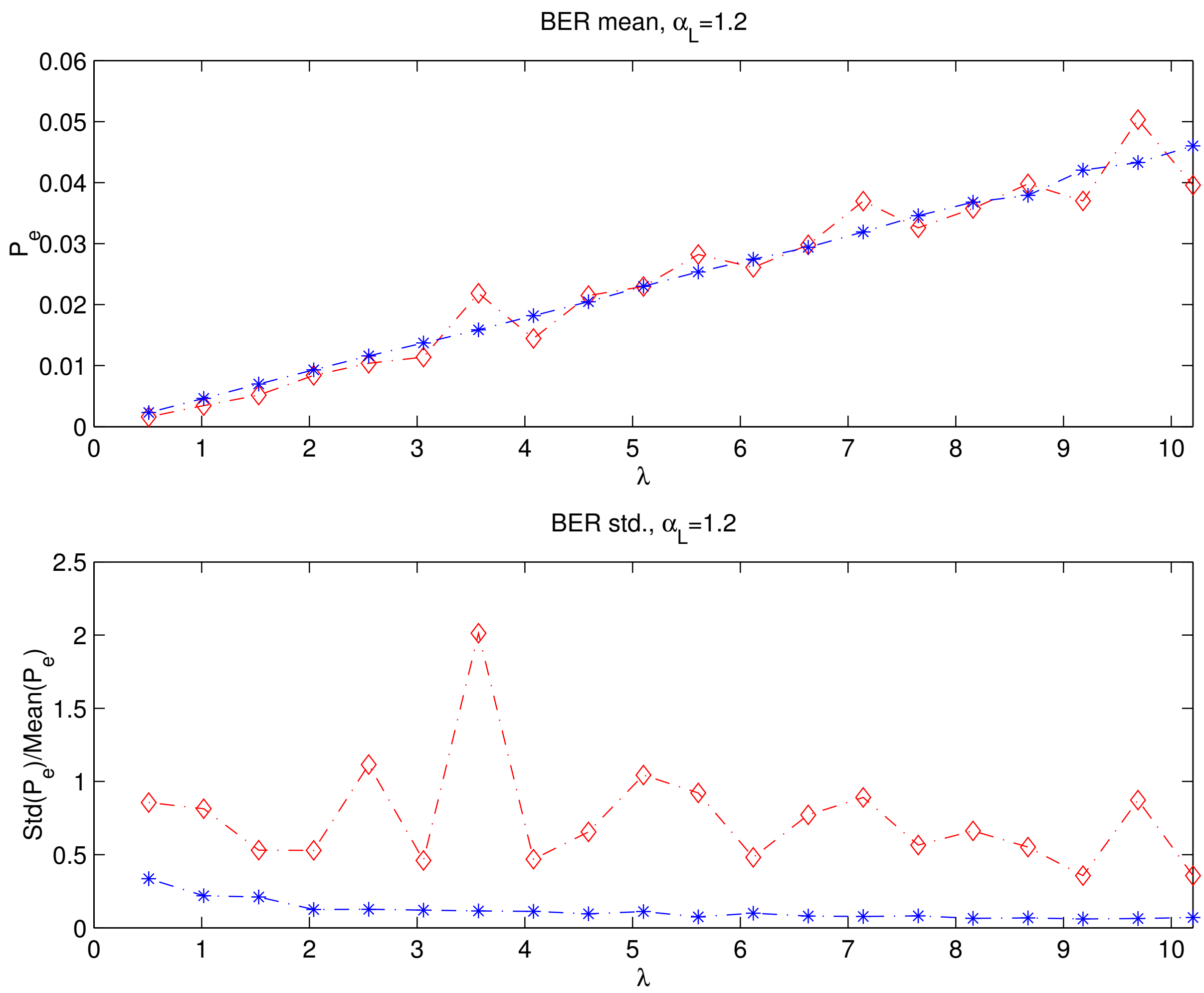

Fig. 5. Mean and standard deviation of bit-error-rate of Cauchy receiver in the presence of long-range dependent ($\alpha_L = 1.2$) and i.i.d α-stable noise, for 40 Monte Carlo simulations. Diamond-marked lines represent the long-range dependent case, while star-marked lines denote the i.i.d. case.